Arabian Journal of Geosciences (2020) 13: 328
https://doi.org/10.1007/s12517-020-05310-0

ORIGINAL PAPER

Characteristics of lava-sediments interactions during emplacement of mid-Tertiary volcanism, Northeastern Desert, Egypt: field geology and geochemistry approach

Hatem M. El Desoky[1] · Taher M. Shahin[1]

Received: 1 September 2019 / Accepted: 31 March 2020 / Published online: 22 April 2020

Abstract

Mid-Tertiary volcanism in the Northeastern Desert of Egypt was associated with the African-Arabian plate rifting and opening of the Red Sea, a period of 30 Ma (Late Oligocene). The resulted lava flows, predominately basaltic sheets, have mingled with the underlying sediments, forming peperite along the contact between them. Field geology, petrography, and geochemistry methods have been used to identify the behavior of the lava-sediment interaction which produced peperite. Two types of peperite have been recognized, fluidal at Naqb Ghul and El-Yahmum areas, and blocky at El-Qattamiya area. Sometimes, the two types are represented together at the El-Qattamiya area. Fluidal peperite is characterized by globular and equant juvenile clasts and with irregular or ragged margins suggesting low viscosity, ductile fragmentation, and sediment fluidization. Blocky peperites are characterized by angular, polyhedral, platy juvenile clasts and a jigsaw-crack texture, resulted from quenching of magma in a brittle regime. The coexistence of fluidal and blocky clasts together reflects progressive disintegration and suggests decreasing temperature and increasing viscosity during fragmentation. The presence of sediments in vesicles and in fractures in the peperite zone indicates a non-explosive phase of interaction. Geochemical data suggests that different composition across the magma/sediment boundary is a result of silicification and sediment fluidization.

Keywords Peperite · Lava/sediment interaction · Oligocene · North Eastern Desert · Egypt

Introduction

Volcanic activities in the middle and northern parts of Egypt were originally spatially associated with the Late Oligocene opening of the Rea Sea (Meneisy and Abdel Aal 1983; Issawi et al. 1999). The volcanics are represented mainly in the form of flood basalts, sheets, sills, dikes, and cinder cones. The interaction between lava and wet unconsolidated sediment commonly forms accumulative sequences of clastic rocks known as peperite, where volcanism takes along sedimentation. Peperites are formed by the dynamic mixing of the quenched debris and the sediments (Cas and Wright 1987). Peperite is essentially formed in situ by the disintegration of magma intruding and mingling with unconsolidated or poorly consolidated, typically wet sediments (White and McPhie 2000). The term also refers to similar mixtures generated by the same processes operating at the contacts of lavas and other hot volcaniclastic deposits with sediments (Skilling et al. 2002). Peperite is commonly formed under submarine environments (Brooks et al. 1982; Busby-Spera and White 1987; Skilling et al. 2002; Wohletz 2002; Martin and Németh 2007; Németh and White 2009). Peperites are often thought to be formed due to the presence of water within the unconsolidated sediments. However, examples from arid environments demonstrate that peperite-forming processes are diverse and may not always require water (Jerram and Stollhofen 2002). De Goër (2000) applied the term peperite for any rock that comprises juvenile glassy volcanic components in a non-juvenile matrix. Peperite is found in different tectonic settings such as intra-continental and arc-related regimes (Németh and Martin 1999; Skilling et al. 2002), commonly associated with intrusions in submarine sedimentary sequences (Brooks et al.

Responsible Editor: Domenico M. Doronzo

✉ Taher M. Shahin
taher_gc@azhar.edu.eg

Hatem M. El Desoky
heldesoky@azhar.edu.eg

[1] Geology Department, Faculty of Science, Al-Azhar University, PO Box 11884, Cairo, Egypt

1982; Busby-Spera and White 1987; Goto and McPhie 1996; Doyle 2000; Dadd and VanWagoner 2002; Kano 2002), lacustrine successions (Cas et al. 2001), lavas (Schmincke 1967; Rawlings et al. 1999; Jerram and Stollhofen 2002), and at the base of pyroclastic flow deposits (Leat 1985 and Branney 1986) in subaerial successions. Peperite is morphologically described as either blocky or fluidal (globular) juvenile clasts (Busby-Spera and White 1987). Non-explosive magma-coolant interactions change where blocky and globular particles have been resulted from significant hydrodynamic magma-coolant mingling (Schipper et al. 2011). The presence of fluvial and lacustrine deposits at the time of lava emplacement suggests that the sediments were remained considerably water saturated, allowing the sediments to be effectively fluidized (McLean et al. 2016). Blocky peperite is characterized by polyhedral, juvenile clasts and jigsaw puzzle texture, whereas fluidal peperite is characterized by fine to very fine juvenile clasts with irregular margins. The study of peperites is important for understanding the mechanisms of lava/sediment interaction, hydro-magmatism, and paleoenvironmental reconstruction. This paper deals with identifying the composition, shape, size, texture, occurrences, and geochemical characteristics of peperite in the study area.

Regional geology

The study district is located at the eastern part of Cairo city and extends from the Cairo-Suez road to Cairo-Sukhna road (Fig. 1), between latitudes 29° 34′ N to 30° 00′ N and longitudes 31° 38′ E to 31° 55′ E, and covers approximately 800 km^2. The district is represented by an unstable continental shelf and was subjected to active extensional deformation and volcanism related to the tectonics of the Gulf of Suez and the opening of the Red Sea since the Oligocene to the Middle Miocene period. The Oligocene climate represents a rainy tropical paleoenvironment conditions that are indicated by the

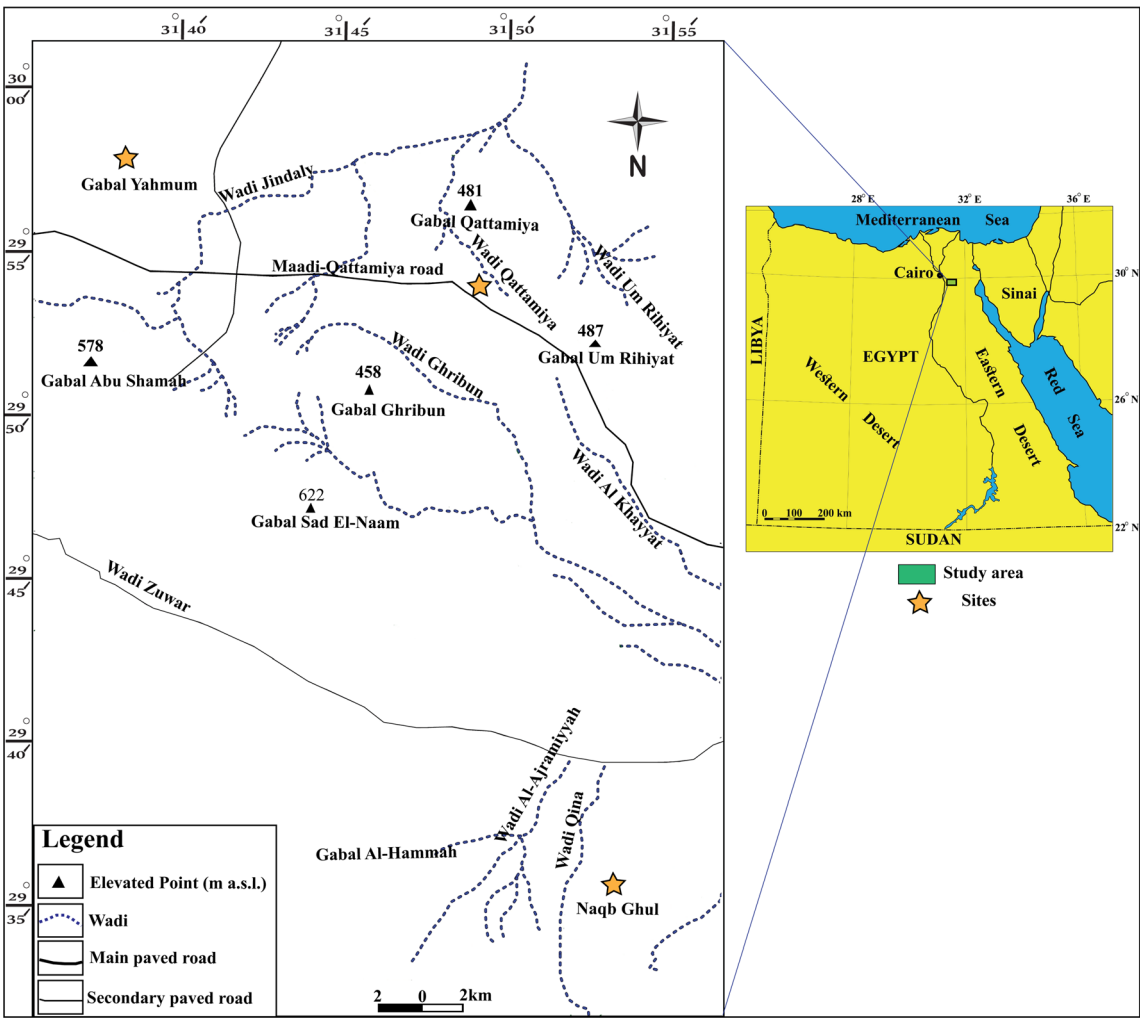

Fig. 1 Location map of the study area and general topographic features with location of the three studied sections, El-Yahmoum, Naqb Ghul, and El-Qattamiya

presence of huge silicified tree trunks, fluvio-lacustrine fossils, quartz, chert, and flint deposits (Abdel Rahman and El-Baz 1979; Said 1990; Embabi 2018). Most of the study rock units are traversed by major normal faults that have a NW-SE trend and often coincide with the main trend of the Gulf of Suez (Moustafa and Abd-Allah 1991). Topographically, the area is controlled by the structures and lithological characteristics that comprise plateaux, wadis, lowland, and isolated hills (Fig. 1).

The study region includes rock assemblages of Eocene strata, composed of limestone, Oligocene rocks (divided into gravels and sands at the base), and rift-related basaltic sheets at the top; Miocene strata, composed of loose sands with small pebbles; Pliocene strata, made up of conglomeratic sands; and Quaternary sediments (Fig. 2). The Eocene strata comprise large exposure of the mapped area and consist of the Maadi Formation (fossiliferous sandy limestone) and the Mokkatum Formation (white

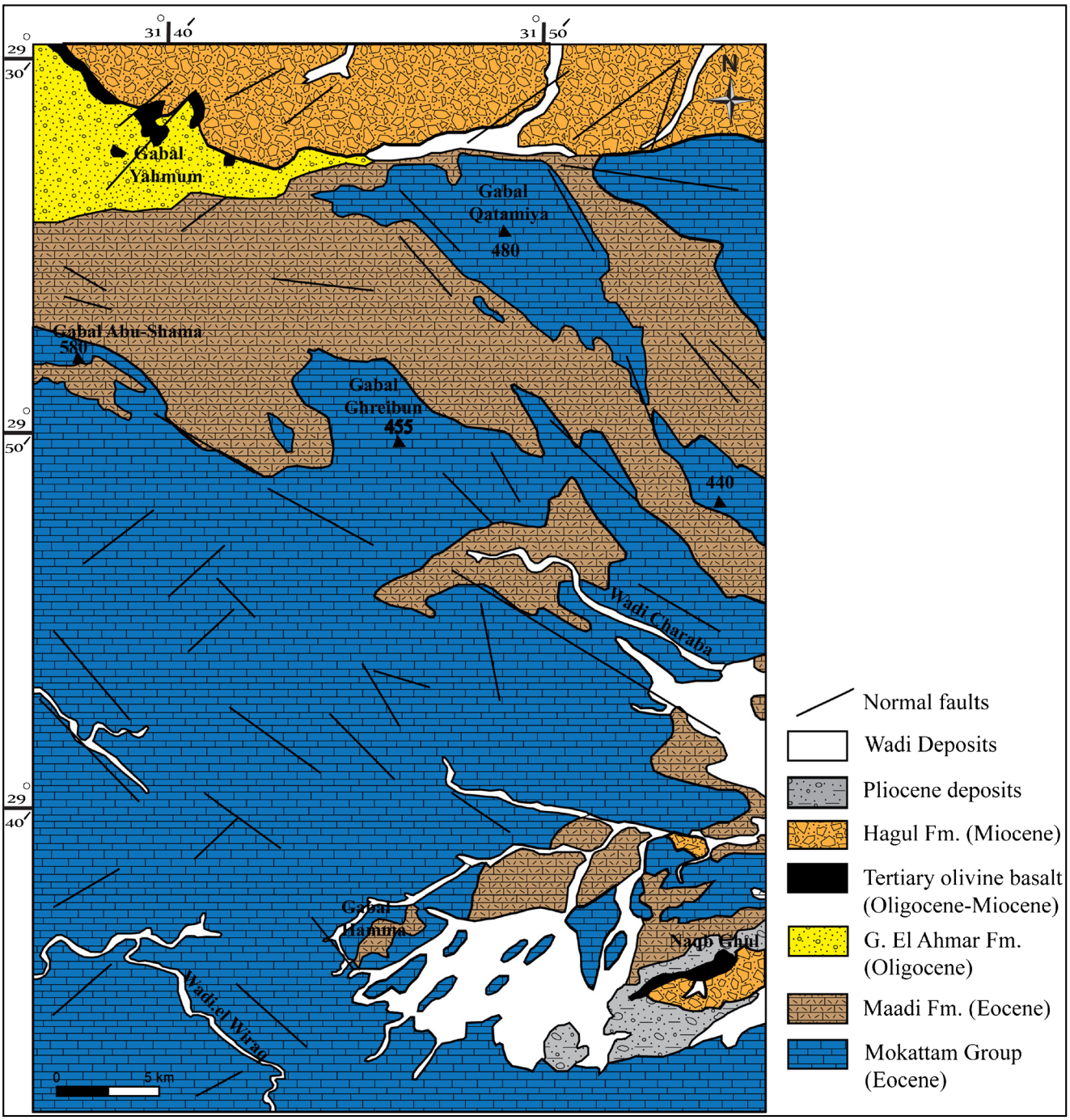

Fig. 2 Geologic map of the study area, North Eastern Desert, Egypt (modified after Conoco 1987)

limestone with *Nummulites gizehensis*). The Oligocene exposes sediments that occur as varicolored, poorly consolidated, and cross-bedded sands and gravels, which were deposited in a fluvial environment and covered by a complex mixture layer of volcanic clasts and sediments (peperite). Meanwhile, they are overlain by volcanic rocks that form a huge sheet of basaltic to basaltic andesite flows, of a pahoehoe lava type, and formed under subaerial conditions. Basalts have been dated using K/Ar techniques at 22–23 Ma (Late Oligocene and Early Miocene) (Meneisy and Abdel Aal 1984).

Stratigraphy

Peperite occurs in excellent three exposures at Naqb Ghul, Gabal El-Yahmum, and El-Qattamiya (Figs. 1 and 3). Relatively simple sequences of stratigraphic units are described as follows.

Naqb Ghul lithostratigraphic sequence forms 24-m-thick dark brown low hills, equivalent to the Gabal Ahmar Formation. It is made up of basaltic rocks and unconformably overlies the Oligocene sediments (Fig. 4a). Sediments commonly display planar and ripple cross-lamination and

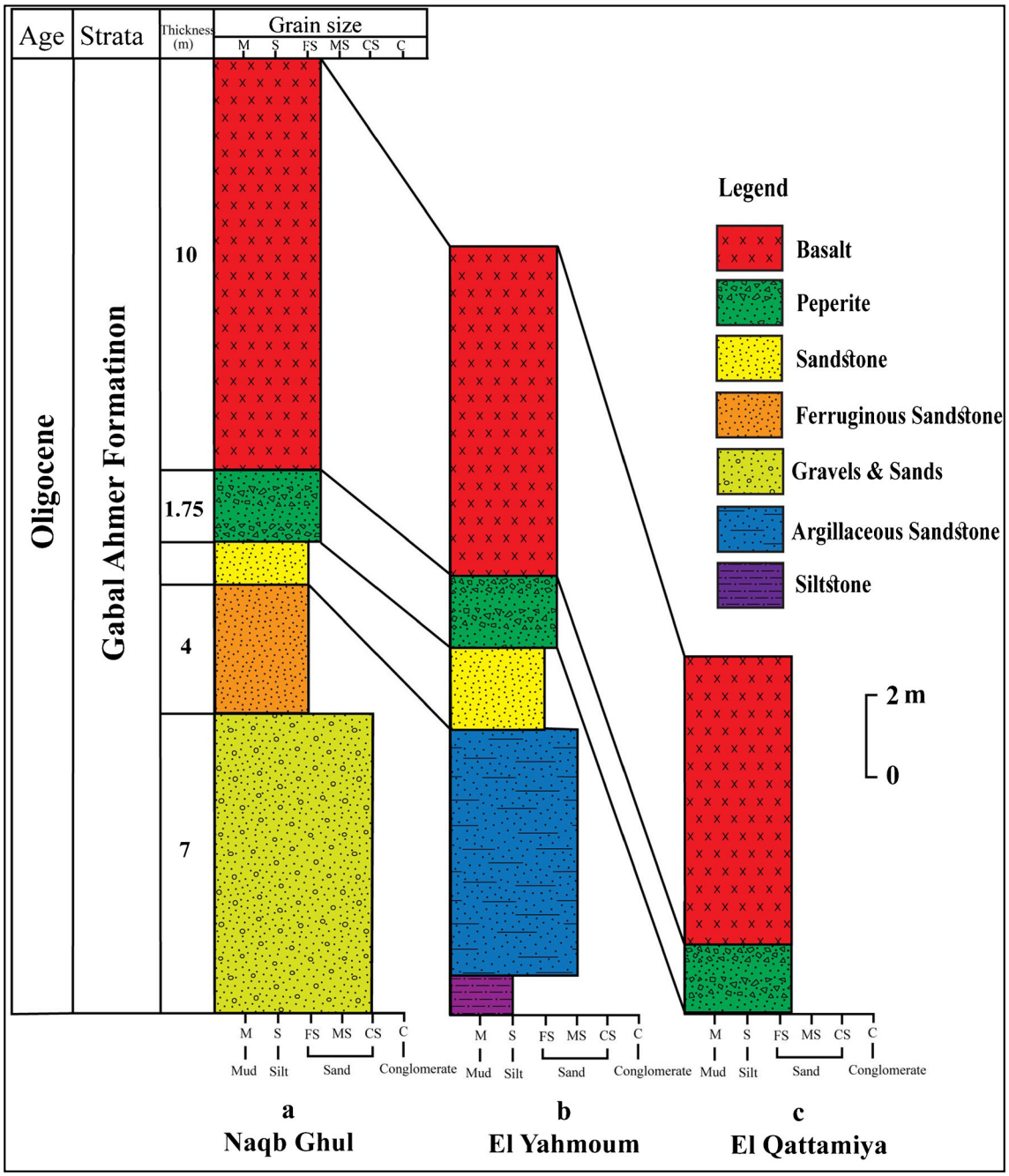

Fig. 3 Lithostratigraphic columns of Oligocene succession in study area

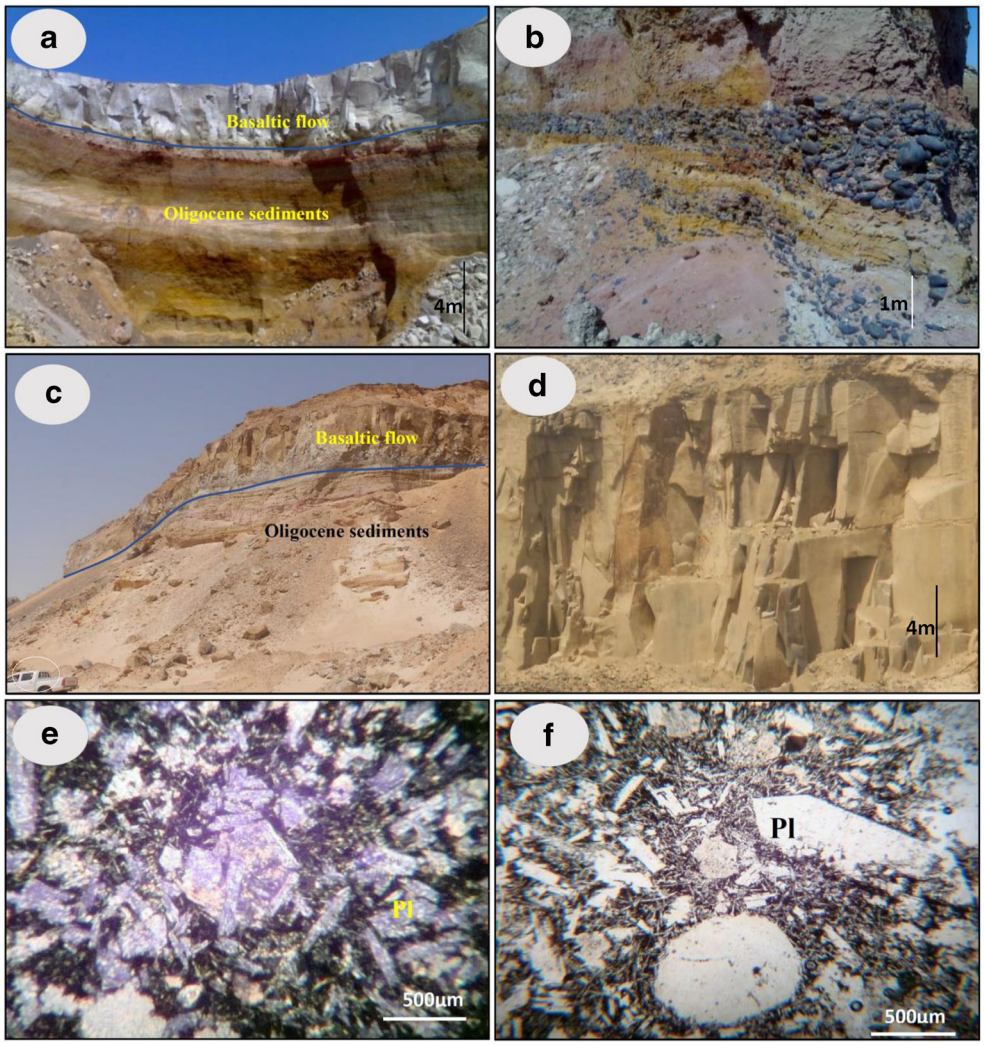

Fig. 4 **a** Photograph showing basaltic flows are overlaying Oligocene sediments at Naqb Ghul area. **b** Sands and gravels of Gabal Ahmar Formation at Naqb Ghul area. **c** Photograph of basaltic flows are overlaying Oligocene sediments at Gabal El-Yahmum. **d** Columnar jointed basalt at Gabal El-Yahmum. **e** Photomicrograph of plagioclase (Pl) lathes slightly altered and impeded in fine-grained groundmass in basalt (C.N.). **f** Phenocrysts of plagioclase (Pl) forming porphyritic texture in basaltic andesite (PPL.)

essentially consist of sands and gravels. The sediments show cross-stratification that illustrated by changes in colors (from reddish-brown, yellow, to black in the lower part) (Fig. 4b). The middle part is composed of siltstone with less commonly claystone and occasionally intercalated with sandy siltstones. Basalts are characterized by medium and fine-grained crystals and composed of plagioclase, pyroxene (augite), olivine, and iron oxides. Plagioclase occurs as subhedral tabular phenocrysts, up to 5 mm in length, set within an aphanitic to intergranular groundmass, and generally shows ophitic to subophitic textures (Fig. 4e).

Gabal El-Yahmum comprises a section, up to 21 m thick, of basaltic flows which overlies the Oligocene clastic sediments, especially in the eastern part (Fig. 4c). It mainly consists of loose sands in the lower part, while the middle part is dark gray sandy, slightly calcareous, and argillaceous sandstone. Some silicification and multi-ferrugination processes occur especially in near fault planes due to the uprising of silica and iron-bearing fluids. The upper part is made up of black, hard basaltic flows, up to 8 m thick, which form a succession of three texturally different zones with characteristic different field appearances. They are designed as a lower zone (A), middle zone (B), and upper zone (C). The lower and upper zones are characterized by amygdaloidal and vesicular textures and mostly intensely altered, while the middle sheet is massive, compact, and mainly fresh (Hassaan et al. 2004 and El-Desoky et al. 2015). Basalt is fine-grained and dark gray in color and shows a well-developed columnar jointing (Fig. 4d).

El-Qattamiya area is truncated by numerous faults and usually composed of lava flow resting unconformably on the Oligocene sediments along Maadi-Qattamiya asphaltic road. The sediments are mainly sands and gravels which form dark brown and black low hills. The lava flow has a thickness ranging from 1 to 8 m, basaltic andesite in composition, and often shows porphyritic texture, as well as amygdaloidal texture. Basaltic andesite consists of plagioclase, olivine, and augite as phenocrysts embedded in a fine-grained groundmass of the same composition. Epidote and calcite are the main

secondary minerals that filled amygdales. Plagioclase shows a tabular to prismatic shape, up to 0.5 cm in length, and mainly of labradorite to andesine in composition. It is also partly to completely replaced by carbonate and epidote minerals (Fig. 4f). Augite is partly replaced by chlorite which occurs as fine-grained aggregates.

Materials and methods

Fieldwork involved the measurement of three sections from different localities which are El-Yahmoum, El-Qattamiya, and Naqb Ghul (GPS coordinates for section 31° 40′ 01″ E, 29° 58′ 30″ N; 31° 40′ 01″ E, 29° 58′ 30″ N; and 31° 40′ 01″ E, 29° 58′ 30″ N, respectively). Photography of critical structures in the field and collection of samples for subsequent laboratory and petrographic analysis were done.

Fourteen representative bulk samples were vertically collected (from the coherent lava, magma-sediment interface peperite, up to the Oligocene sediments) with distance up to 50 cm from the studied area, which may reveal significant data about the geochemical compositions. Peperite samples comprise a mixture of volcanic clasts, siliciclastic sediments, of fine grain-size that is difficult to separate volcanic clasts for analysis.

Whole-rock samples were crushed in a hydraulic press and then pulverized using an agate mill in the Department of Geology, Faculty of Sciences, Al-Azhar University, Egypt. Samples were analyzed for both major and trace elements. The major oxides were analyzed by using X-ray fluorescence (XRF) spectrometer. The content of trace elements was estimated by ICP analysis. The analysis has been carried out in the Institute of National Research Center laboratories, Egypt. The analytical results are presented in Table 1.

The peperite samples were examined by X-ray diffraction (XRD) pattern to identify the mineralogical composition and the semi-qualitative content of the minerals. The XRD technique is a non-destructive, very versatile technique to determine the crystalline phases and their volume fractions. The examined samples were prepared for analysis as follows.

In this technique, the studied samples were prepared by fine grounding to 20 μm using HERZOG (Herzog Co., Germany) grinder, to minimize the effect of absorption and extinction of the X-ray beam. Rectangular type sample holder was used to pack about 0.2 g of the examined samples. The sample holder is then fed into the Pan Analytical X, Pert Properties MPD PW 3050/60 X-ray diffractometer, provided with a proportional digital counter and Nickel-filtered Cu-Kα radiation at 40 kV and 30 mA, over an interval of 5–50° at a scanning speed of 5°/min. The XRD patterns obtained were converted to a series of lattice spacing (Å). The XRD pattern data obtained were identified by computer software "X' part High Score" using PDF cards of International Center of diffraction Data (ICDD 2006).

Results

Peperites

Peperites are formed at the contacts between basalts and the sedimentary host rocks due to disintegration and fragmentation of magma. They are commonly characterized by clastic textures, from blocky shaped igneous clasts to globular igneous bodies, both are dispersed and usually indurated sedimentary rocks. Peperite is manifested in three excellent exposures at Gabal El-Yahmum, Naqb Ghul, and El-Qattamiya (Figs. 2 and 3).

Fluidal peperites

Fluidal peperites are the dominant type at Naqb Ghul and Gabal El-Yahmum. The contacts between basaltic lava and unconsolidated sands are commonly irregular characterized by the development of globular/fluidal peperite zone, up to 1 m thick. The juvenile clasts with unconsolidated sediments are rounded to subrounded, with a size ranging from 1 to 3 cm, and generally display closely packed clasts (Fig. 5a, b). In thin sections, fluidal clasts have bulbous, globular shapes that are more abundant and irregular morphologies, (Fig. 5c).

Fluidal peperite zones often contain vesicles which are dispersed. Vesicles are sometimes connected together by thin necks and filled with carbonate and quartz minerals (Fig. 5d). The presence of vesiculation probably suggests degassing of primary magmatic volatiles and injection of steam from external water prior at the lava-sediment interface (Hunns and McPhie 1999; Doyle 2000).

The host sedimentary matrix is reddish-brown sands and minor siltstone. Sand matrix is dominated by quartz, feldspar, and opaque minerals. Sands are represented by well-rounded grains, sometimes with no significant chilled margin. The rounded to subrounded quartz grains are morphologically preserved (Fig. 5e), and partly fill the interstitial spaces along with carbonate and fine clay flakes in peperite. Generally, close to the contact with peperite zone recrystallized quartz is observed, in thin-sections, and indicated by contact metamorphism. (Fig. 5f).

Blocky peperites

Blocky peperites only occur along the base of basaltic flow in El-Qattamiya area (Fig. 6a). Peperite zone has a sharp boundary against underlying sediments, and with a thickness ranging from 1 to 2 m. They are represented by basaltic juvenile clasts, commonly close-packed, angular in shape, and also have cracks and vesicles which are filled with sediments. Blocky clasts have polyhedral and cuneiform shapes with gently curved margins, which form a jigsaw-fit texture (Fig. 6b, c). Microscopically, juvenile clasts are

Table 1 Representative chemical analyses for major oxides (wt.%) and trace elements (ppm) of the studied peperite samples, primary basaltic lava and Oligocene sediments

S. no. of oxides (wt.%)	Basalt			Peperites									Sandstone	
	1H	1Q	1Nq	2H	3H	4H	5H	2Q	3Q	3Nq	4Nq	5Nq	1H	1Nq
SiO_2	45.03	43.37	45.48	66.87	46.15	61.97	51.79	34.65	38.60	43.35	35.96	50.12	80	69.05
TiO_2	3.15	3.97	2.62	2.01	0.71	2.24	4.07	3.81	3.59	4.39	4.43	2.94	1.13	1.17
Al_2O_3	15.76	16.07	13.65	15.98	3.57	17.28	18.23	15.74	17.61	15.90	16.33	10.10	6.41	9.33
FeO	5.23	5.14	5.76	4.17	2.96	5.32	8.83	15.73	9.27	14.92	16.68	17.08	2.06	6.45
Fe_2O_3	10.37	11.56	16.64	2.79	1.19	3.22	4.72	6.60	6.54	6.64	6.63	8.16	1.54	4.03
MnO	0.18	0.25	0.18	0.34	0.18	0.63	1.00	0.36	0.22	0.68	0.31	0.43	0.18	0.21
MgO	2.58	3.31	2.49	1.97	0.65	2.29	2.77	3.25	1.96	2.42	1.76	1.33	0.90	1.60
CaO	11.40	11.93	10.09	1.30	40.2	1.47	2.20	12.67	4.03	6.16	12.8	6.26	2.37	4.02
Na_2O	2.04	1.97	1.58	1.31	0.63	1.45	1.71	2.20	6.88	1.01	0.98	0.99	0.15	0.67
K_2O	1.42	0.57	0.18	0.96	0.37	0.65	1.04	1.44	1.37	1.54	1.90	0.96	0.91	0.46
P_2O_5	0.55	0.54	0.53	0.19	0.09	0.29	0.60	0.30	0.13	0.36	0.30	0.21	0.12	0.24
SO_3	0.14	0.15	0.20	0.08	0.97	0.10	0.14	0.32	0.09	0.65	0.12	0.06	0.41	0.13
Cl	0.54	0.53	0.03	1.42	0.74	1.43	2.16	1.42	7.14	1.13	0.51	0.02	2.71	1.47
F	0.00	0.00	0.00	0.00	0.00	0.00	0.00	0.00	0.00	0.00	0.00	0.00	0.00	0.00
L.O. I	0.62	0.62	0.65	0.56	0.61	0.71	0.66	0.64	1.73	0.61	0.84	0.58	0.62	0.45
Total	99.01	99.98	100.	99.96	99.0	99.06	99.92	99.13	99.15	99.77	99.60	99.23	99.73	99.28
Trace elements (ppm)														
Sr	120	210	390	600	112	570	102	540	280	240	212	114	300	410
Cr	100	100	110	300	300	300	100	200	100	200	200	200	200	300
Ni	93	50	110	9 0	40	80	97	60	70	90	153	60	30	40
V	300	310	323	347	170	462	122	220	310	121	118	144	44	110
Co	168	142	122	77	71	147	144	152	130	144	145	146	152	154
Cu	169	114	100	28	100	47	100	100	200	100	100	100	100	42
Y	127	89	40	105	100	200	100	59	120	31	62	200	100	42
Pb	83	210	37	100	128	200	95	130	220	310	200	210	100	230
Nb	40	47	41	120	40	50	50	57	60	64	80	50	60	20
Zr	130	200	190	160	143	120	160	150	173	107	202	133	24	200
Ga	100	79	40	100	100	200	200	200	100	123	138	200	100	200
Zn	150	189	130	25	21	150	240	128	160	220	330	250	210	210
La	39	37	41	6	30	80	40	57	30	60	40	60	50	50
CIA	51.47	52.62	53.53	81.74	7.97	82.88	78.65	49.11	58.92	64.61	51.02	55.16		

LOI loss on ignition, *CIA* CIA = $[Al_2O_3/(Al_2O_3 + CaO^* + Na_2O + K_2O)] \times 100$, *H* El-Yahmum, *Q* Qattamiya, *Nq* Naqb Ghul areas, *1H* yellow loose sands, *1Nq* ferruginous loose sandstones

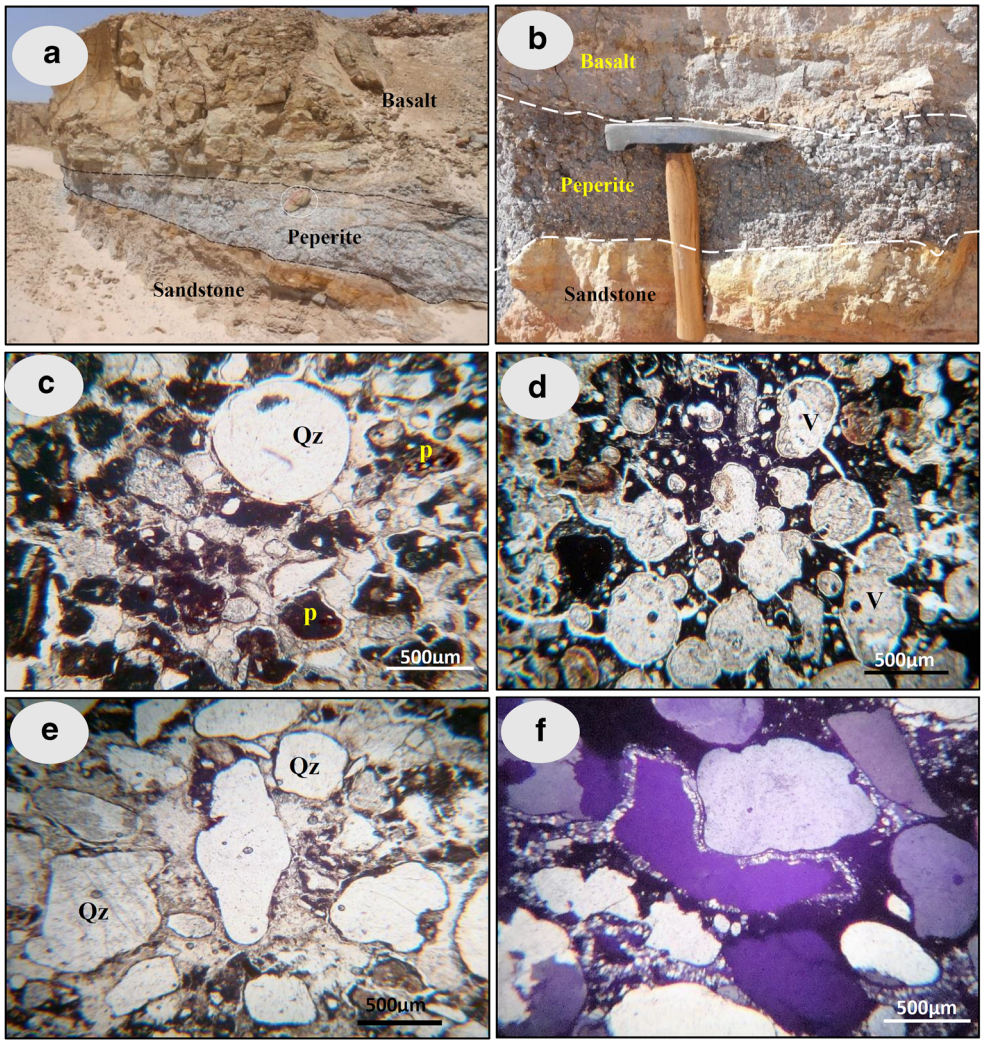

Fig. 5 Photographs showing the lava/sediments interactions. **a** Peperitic contact zone at the lower contact of the basalt with sandstone as a host rock in the Gabal El-Yahmum. **b** Microglobular peperite jointed and closed-packed of juvenile clasts within the host sediment in the Naqb Ghul area. **c** Photomicrograph showing irregular juvenile basalt clasts of fluidal (P) type with quartz (Qz)-filled cavities (PPL.). **d** Vesicles (v) appear spherical connected by thin necks and are filled by carbonate (PPL.). **e** Subrounded quartz (Qz) clasts characterized by no chilled margins and preserved shapes in peperite zone (PPL). **f** Photomicrograph showing recrystallized quartz along contact of the lava/sediments (PPL.)

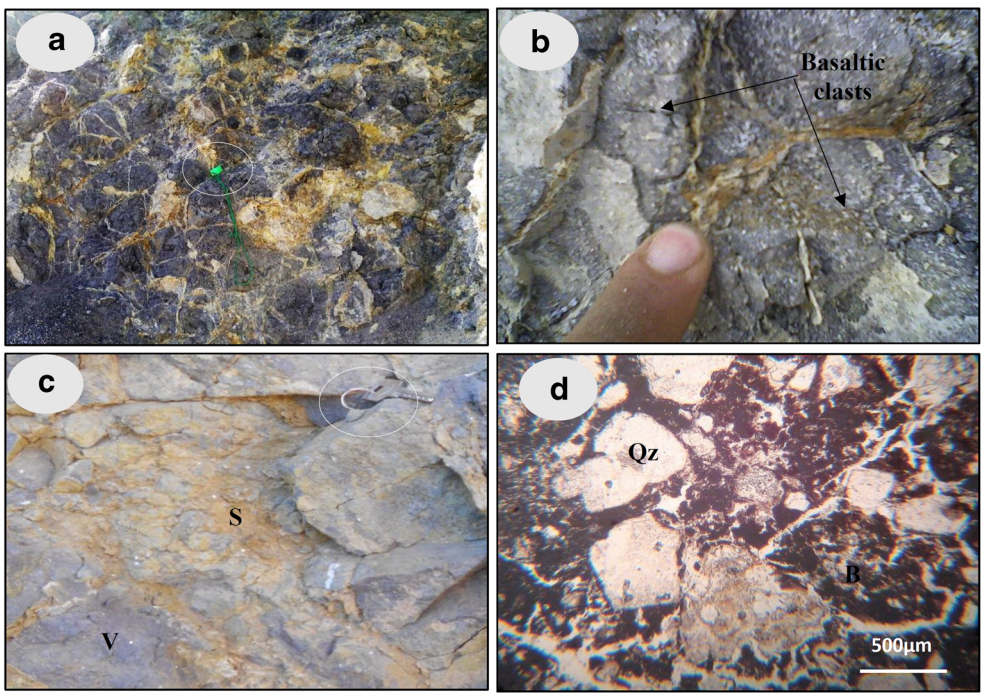

Fig. 6 Photographs showing the lava/sediments interactions. **a** Blocky peperite developed along wadi Qattamiya. Note that basalt is dark, and host sandstone with carbonate is white. **b** Close-up view shows well-developed jigsaw-fit texture in blocky peperite. **c**. Irregular blocky volcanic clasts (V) of basalt in a sedimentary matrix (S) in Qattamiya area. **d** Well-developed micro-blocky peperite (B, sideromelane) with tabular morphology and jigsaw fit structure with quartz (Qz) grains (PPL.)

characterized by angular to subrounded in a solidified sandy matrix, and range in size from 0.5 to 2 mm (Fig. 6d). Sometimes, clasts show mixed morphologies of both blocky and fluidal (globular) clasts.

Mineralogical and geochemical aspects

XRD analyses have been carried out on the peperite samples, which were collected from three different localities: at Naqb Ghul, El-Yahmoum, and El-Qattamiya areas, to estimate their mineralogical composition. The XRD patterns of the various peperite samples indicate that they mainly consist of quartz (characteristic peak at 3.34 Å, 4.26 Å, and 1.82 Å), montmorillonite (characteristic peak at 14.9 Å and 12.2 Å), calcite (characteristic peak at 3.35 Å, 3.84 Å, and 2.09 Å), and hematite minerals. Small amounts of anorthoclase and cristobalite minerals have been detected in El-Yahmoum and Naqb Ghul samples (Fig. 7). The bulk mineralogy of the

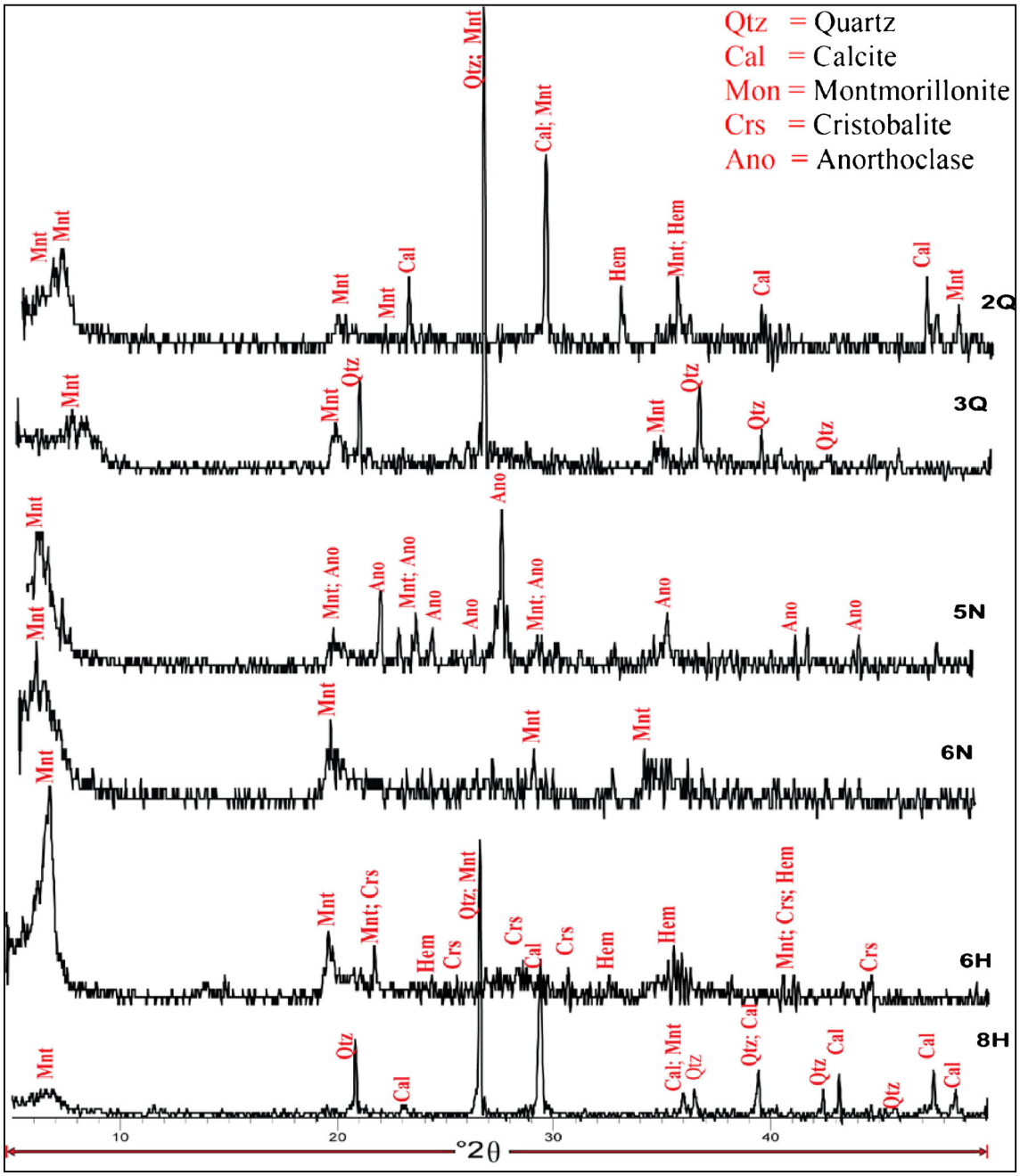

Fig. 7 X-ray diffraction analysis. (2Q, 3Q) mineralogical composition of peperite is calcite, montmorillonite, quartz, and hematite at Gabal El-Qattamiya. XRD patterns of peperite sample no. (5N) of Gabal Naqb Ghul. Peperite (6H, 8H) showed six minerals represented by calcite, montmorillonite, quartz, hematite, and cristobalite in Gabal El-Yahmoum

samples, as revealed by the X-ray diffraction, is the same as of the sediments filling the interstices between basaltic clasts. The mineralogical assemblages of the peperitic domain are characterized by the presence of siliciclastic matrix and the absence of fine volcanic ash that is the evidence for non-explosive fragmentation during the emplacement of lava. This was used to distinguish the peperite textures from the textures of volcaniclastic rocks formed by explosive eruptions (Nemeth and White 2009).

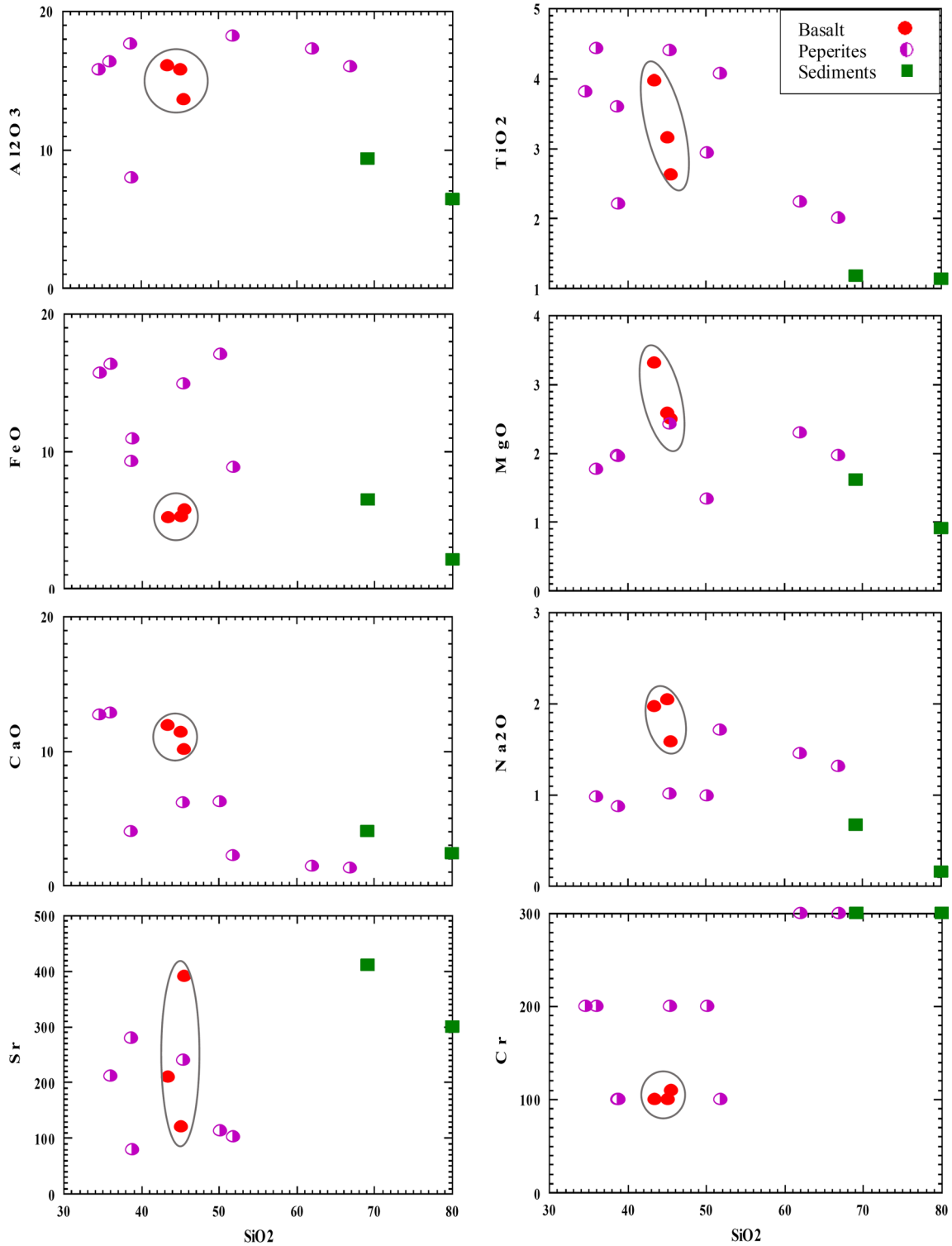

Fig. 8 Variation diagrams for selected major element oxide and trace elements versus SiO_2 of the coherent lava (basalt), peperites, and Oligocene sediment samples of the studied area

Representative bulk chemical compositions of the basaltic lava, Oligocene sediments, and peperite rocks are shown in Table 1. Variation diagrams show that the majority of major oxides of the basalt are declined with increasing silica (Table 1 and Fig. 8). Moreover, the basaltic rocks have a chemical affinity of tholeiite to alkaline nature developed within the plate continental rift associated with the Gulf of Suez rift basin (El-Desoky et al. 2015). Sedimentary rocks are characterized by silica contents range from 69.05 to 80 wt.% for sandstones. Silica is negatively correlated with Al_2O_3, TiO_2, CaO, MgO, FeO, and Na_2O, whereas Cr is positively correlated (Fig. 8). Generally, the difference in the composition between coherent lava and sediments along lava/sediment boundary is clearly visible by Si and Al content (basalt: $SiO_2 = 56.9$ wt.%, $Al_2O_3 = 15.67$ wt.%; sandstone: $SiO_2 = 69.05$ wt.%, $Al_2O_3 = 1.13$ wt.%), which probably suggest elements mobility and silicification process as a result of peperite formation (Kokelaar 1982).

The investigated peperites show large ranges in major oxide concentrations as compared with basaltic lava (SiO_2 61.97–34.65 wt.%; Al_2O_3 17.28–3.57 wt.%; TiO_2 4.39–0.71 wt.%; Fe_2O_3 8.16–1.19 wt.%; FeO 17.08–2.42 wt.%; MgO 3.25–0.65 wt.%; CaO 40.2–1.30 wt.%; Na_2O 6.88–0.63 wt.%; K_2O 1.44–0.31 wt.%). The high silica content is probably related to post-magmatic silicification. Variation diagrams (Fig. 8) show that most of the major oxides, of the primary volcanic rocks in comparison with the associated peperite, are decreasing with increasing silica, while Na_2O and K_2O increase when SiO_2 increases. The higher content in both SiO_2 and CaO in the El-Yahmoum area is greater than in the El-Qattamiya and Naqb Ghul areas, maybe as a result of major element mobility during mingling of lava with sediments. Meanwhile, Na_2O and K_2O are higher in the El-Qattamiya area (more felsic samples) rather than the other two sections of El-Yahmoum and Naqb Ghul, thus indicating that Na was probably the most mobile of the alkalis.

The chemical analyses of the trace elements, from the peperite zone, revealed some differences when compared with primary basalt samples Table 1. Generally, almost all of the trace elements show a broad scatter of linear trend correlation with SiO_2, while Sr and Cr are increased with SiO_2 increase (Fig. 8). The concentrations of the ferromagnesian element Ni are medium, averaging 69 ppm. Meanwhile, the concentrations of most high field strength elements are particularly high (e.g., Nb average is 63 ppm, Zr average is 152 ppm, Y average is 103 ppm, Cr average is 200 ppm). The general higher concentration of the ferromagnesian element particularly Cr contents in peperite zone may reflect a stronger mafic igneous contribution to these rocks.

The relative concentrations of the Chemical Index of Alteration (CIA) are shown in A-CN-K trinary diagram (Fig. 9a) proposed by Nesbitt and Young (1984). The CIA value is usually about 50 (for fresh crystalline rocks), more than 60 suggesting lower weathering, 60–80 suggesting moderate weathering, and more than 80 suggesting extreme weathering (Fedo et al. 1995). The CIA values of the studied peperite vary from 7.97 to 64. These results indicate that all the peperite samples, except for three samples (altered), are mainly composed of relatively unweathered materials. The normalized trace elements of basalt and peperite to MORB (Pearce 1983) show a similar trace element profile to the volcanic rocks, with depletions of Zr, Y, and Zn, and enrichment of Nb, V, Cr, and Ni in most samples (Fig. 9b).

Discussion and interpretation of peperites

Igneous activity in the greater Red Sea rift system and environs occurred in distinct phases: (i) volcanism at ~ 46–34 Ma that was documented in the southern Main Ethiopian Rift and with time correlative units in southern Egypt; (ii) continental flood basalts in Ethiopia, Eritrea, South Sudan, and Yemen at

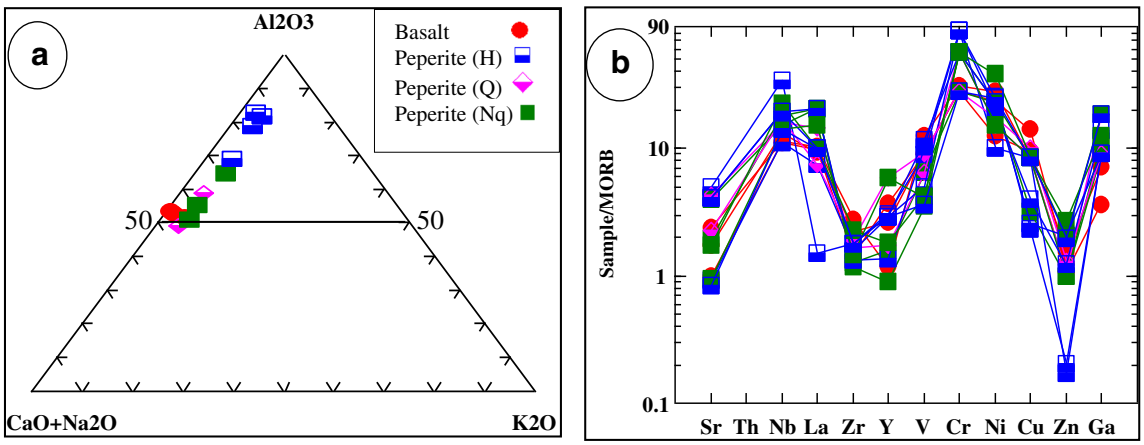

Fig. 9 Geochemical characteristics of the peperite. H, El-Yahmum; Q, Qattamiya; Nq, Naqb Ghul areas. **a** Plots of the basalt and peperite samples on Al_2O_3-(CaO* + Na_2O)-K_2O; (A–CN–K) ternary diagram (Nesbitt and Young 1982). **b** Spider diagram for the study peperite normalized to MORB (Pearce 1983)

31–30 Ma; (iii) eruption of the Marda volcanic zone southeast of Afar, a large extrusive event in northern Egypt, and the Harrat ash Shaam region of Jordan at ~ 26.5–21 Ma; (iv) continued volcanism within Afar (mostly after ~ 20 Ma); and (v) oceanic spreading along the southern axis of the Red Sea no later than 5 Ma (Bosworth and Stockli 2016). Peperites are common, where lava flows traveled through wet sediments (Skilling et al. 2002; Nėmeth 2009). They are the result of the mingling of magma with unconsolidated sediments, which occurs during non-explosive interactions at the margins of intrusive/extrusive igneous bodies. The formation of peperites in the study area is consistent with the Early Miocene Bigadic basin (Western Turkey) mentioned by Erkül et al. (2005), and Balhaf-Bir Ali Plio-Quaternary volcanic field (Arabian Sea, Republic of Yemen) mentioned by Heikal et al. (2012).

The basaltic flows, flowed over the unconsolidated Oligocene sediments, fragmented and disintegrated to form juvenile clasts, were mingled with the host sediments. Fragmentation of lava intruding sediments can be due to several processes, including quenching, mechanical stress, pore-water steam explosions, explosive juvenile vesiculation, and magma-sediment density contrasts. The main mechanism suggested for mingling of the igneous clasts with the sediment is fluidization, in the sense of particle support and transport by a fluid (Skilling et al. 2002). However, the presence of water is not a requirement; fragmentation can also be generated by mechanical processes (the effects of gravity and loading), auto-brecciation of the magma, the expansion of trapped air in pore spaces, and the marked topographical variation found in arid environments (Jerram and Stollhofen 2002). Mingling is favored when the density and viscosity of the magma are like that of the wet sediments, at least locally at the time of mingling (Zimanowski and Büttner 2002). The studied peperite exhibits different textural types, which comprise fluidal, blocky, and mixed textures. Furthermore, fluidal peperites appear in the Naqb Ghul and El-Yahmoum, whereas blocky and mixed peperites (two types) are located at the El-Qattamiya area (Figs. 5a–c and 6; Table 2).

Fluidal peperite has shown that globular textures predominate in the studied areas where lava intruded into sediments, in which vapor films could be maintained at the lava-sediment interface. Fuel-coolant interactions occur when a hot liquid (fuel) contacts a cooler liquid (coolant) whose vaporization temperature is less than the fuel temperature (Busby-Spera and White 1987). Fluidal peperite has been generated during fuel-coolant interactions with tiny and transportable particles of the sedimentary host, viewed as essentially accidental components of the (fluid) coolant. Fluidal peperites suggest a ductile regime, with fragmentation caused by fluid instabilities within vapor films, magma-sediment density contrasts and hydro-magmatic explosions (Busby-Spera and White 1987; Skilling et al. 2002). Fluidization of host sediments plays a significant role in the development of fluidal clasts and mingling. It occurs within the vapor films by heating of magma, or by pressure released during the opening of fractures at the magma-wet sediment interface, which provides space for the intruded magma and drives the sediment particles to move as a fluid along cooling fractures and joints in lava (Kokelaar 1982).

Naqb Ghul peperites recorded such fluidization of wet unconsolidated sediments by basaltic magma, consistent with the field and thin sections observations (Figs. 4c, 5d, and 10a). The main evidence for sediment fluidization is the occurrence of narrow localized contact zones along basalt-Oligocene sediment contacts, destruction of original sedimentary structures, and sediment-filled vesicles near the outer surfaces of clasts (Kokelaar 1982; Kano 1989 and 1991; McPhie 1993; Goto and McPhie 1996; Hanson and Hargrove 1999; Dadd and Van Wagoner 2002).

Blocky peperites are developed by fragmentation of magma in the brittle regime due to the quenching and mechanical stresses, in which blocky juvenile clasts are dispersed in the host Oligocene sediments. Such processes imply a rapid transfer of magmatic heat to the pore fluids. Jigsaw-fit textures of the studied blocky peperites (Figs. 6, and 10b) indicate that the fragmentation of magma is a result of quenching, which directly reflects in situ fragmentation and no further transportation of juvenile clasts (Kokelaar 1986; Hanson and Schweickert 1982; Skilling et al. 2002). Fractures of the jigsaw-fit textures are filled with host sediments that directly indicate the fluidization and movement of sediments into the

Table 2 Simplified summary of the studied peperite types

Locality	Peperites	Host sediments	Igneous rock	Volcanic clasts
Naqb Ghul	Fluidal, close-packed	Sandstone-sand, fine grained, well sorted	Massive basaltic lava flow	Medium-grained globular, vesicular
El-Yahmoum	Blocky, close-packed	Sandstone-sand, fine grained, well sorted	Massive basaltic lava flow	Jigsaw-fit angular, 1–10 cm in size, sparse fluidal and angular mixed, slightly vesicular
Qattamiya	Blocky, close-packed	Sandstone-sand with siltstone, fine grained, well sorted	Massive basaltic lava flow	Jigsaw-fit angular, 1–20 cm in size, slightly vesicular

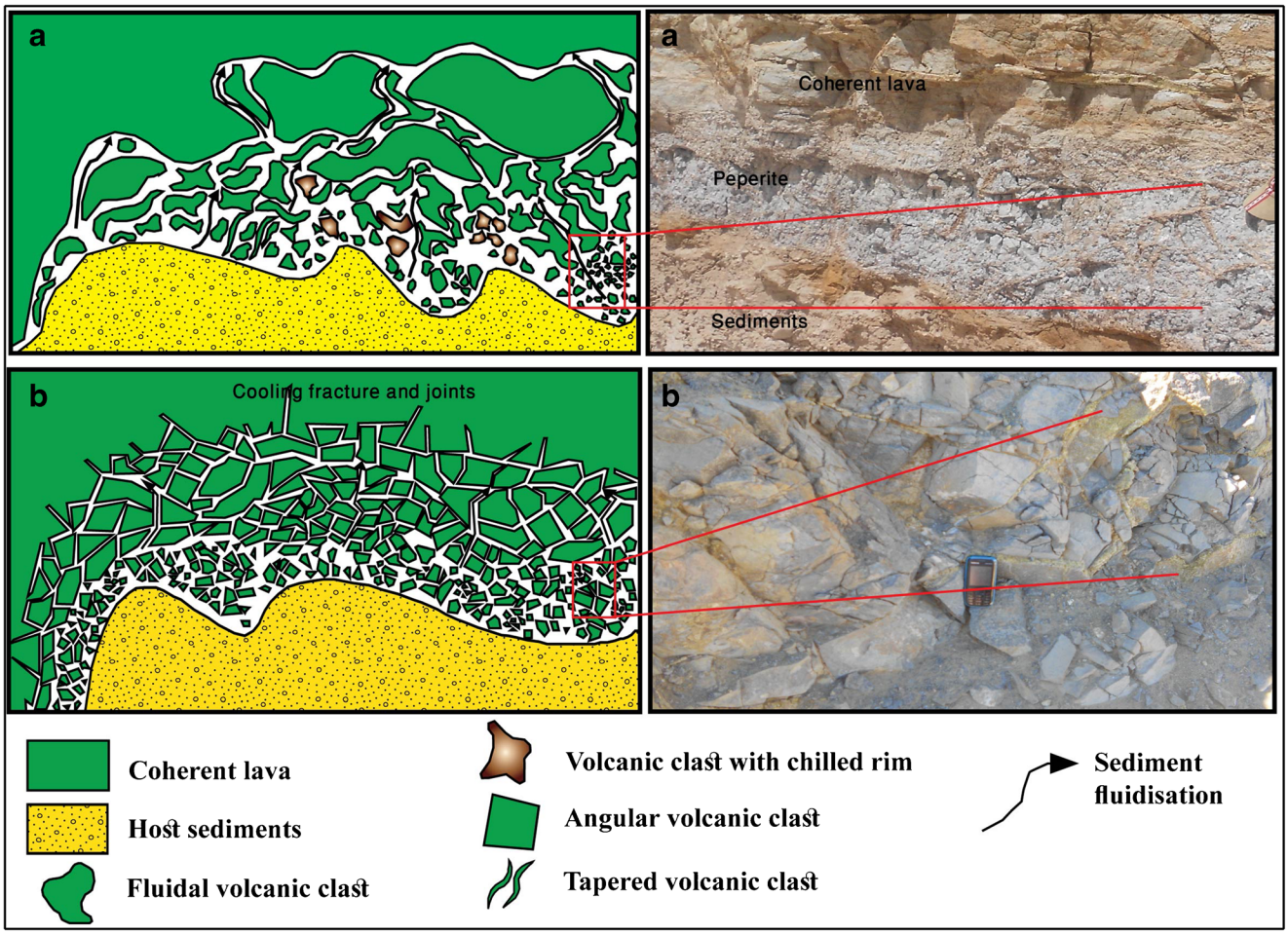

Fig. 10 Simplified schematic diagrams showing the formation of fluidal (**a**) and blocky (**b**) studied peperites

fractures (Brooks et al. 1982; Kokelaar 1982). The fluidized sediments fill the cooling fracture spaces of new fragmented clasts, forming the final pattern of blocky peperites (Hanson and Schweickert 1982; Kokelaar et al. 1986). Usually, the clasts of blocky peperites are closely packed, poorly sorted, and coarse-grained sediments in which insulating vapor films are not preserved.

Sometimes, mixed peperites are found at the El-Qattamiya area. The presence of mixing blocky and fluidal peperites may be developed by the viscosity changes during the cooling and mixing of the magma with wet sediment (Brooks et al. 1982; Chen et al. 2013). The rhyolitic magma of high viscosity only produces blocky peperite. In contrast, the low-viscosity magmas (basaltic) produce a combination of blocky and fluidal peperites (Dadd and Van Wagoner 2002). Mixed globular and blocky peperites suggest a change in fragmentation of ductile regime along with the brittle ones, mixing lava with sediments during interaction. Low-viscosity magma may support the formation of globular peperite, but when their viscosity increases, due to cooling or crystallization, it may instead form blocky peperite across the brittle/ductile transition (Doyle 2000; Skilling et al. 2002).

Conclusion

The volcanic activity at North Eastern Desert is anorogenic continental rifting, represented by flood basalt sheets capping hills of Oligocene sands and gravels. The studied peperites are formed by the mingling of basaltic lava flows with unconsolidated Oligocene sediments. Peperite comprises different features that reflect verity styles of lava-sediment interaction.

Two types of peperites are identified, blocky and fluidal/globular, with different morphologies. Naqb Ghul and El-Yahmoum peperites are represented by fluidal type, which occur as small globular shapes of the basalt clasts hosted in sediments, and are developed at a ductile regime. It shows a relatively low-viscosity behavior of the lava, while a vapor film is insulated in the lava from direct contact with the wet sediments. Meanwhile, El-Qattamiya blocky peperites display angular, polyhedral shapes of basalt clasts and are generated by quenching of somewhat cooler and implying brittle fragmentation. Sometimes, mixed peperites are found at the El-Qattamiya area, suggesting a change in fragmentation of the ductile regime along with the brittle one.

Fluidization is a common mechanism of peperite formation that leads to the mingling of juvenile clasts with sediments at the lava/sediment interface. Sediments in vesicles and juvenile clasts in peperites, along with soft sediment deformation, are the main evidences of the non-explosive phase of interaction.

Geochemical evidence suggests that the enrichment of SiO_2 and Na_2O, with a slight enrichment of K_2O, within the peperite, in the study area, reflects the silicification of the sedimentary matrix due to peperite-driven fluid migration.

Acknowledgments The authors are grateful to Dr. Atef Afifi for his fieldwork assistance. The authors would also like to thank Dr. Alison Graettinger (University of Missouri, KS, USA) for her critical comments. The manuscript was substantially improved by the helpful comments of two anonymous referees and Chief Editor Prof. Domenico Doronzo. Many thanks would go to the Department of Geology (Al-Azhar University) for giving access to laboratories equipped with the needed facilities.

References

Abdel-Rahman M, El-Baz F (1979) Detection of a probable ancestral delta of the Nile River. In: F El-Baz and D M Warner D (eds) Appolo-Soyuz test project, vol II. Earth observations and photography, NASA, Washington DC, pp 511–520

Bosworth W, Stockli DF (2016) Early magmatism in the greater Red Sea rift: timing and significance. Can J Earth Sci 53(11):1158–1176. https://doi.org/10.1139/cjes-2016-0019

Branney M (1986) Isolated pods of subaqueous welded ash-flow tuff: a distal facies of the Capel Curig Volcanic Formation (Ordovician), North Wales. Geol Mag 123:589–590. https://doi.org/10.1017/S0016756800035184

Brooks ER, Woods MM, Garbutt PL (1982) Origin and metamorphism of peperite and associated rocks in the Devonian Elwell Formation, northern Sierra Nevada. California Geol Soc Am Bull 93:1208–1231. https://doi.org/10.1130/0016-7606(1982)93<1208:OAMOPA>2.0.CO;2

Busby-Spera CJ, White JDL (1987) Variation in peperite textures associated with differing host-sediment properties. Bull Volcanol 49:765–775. https://doi.org/10.1007/BF01079827

Cas RAF, Wright JV (1987) Volcanic successions modern and ancient. Allen & Unwin, London. https://doi.org/10.1007/978-94-009-3167-1

Cas RAF, Edgar C, Allen RL et al (2001) Influence of magmatism and tectonics on sedimentation in an extensional lake basin: the Upper Devonian Bunga Beds, Boyd Volcanic Complex, Southeastern Australia. In: White JDL, Riggs NR (eds) Volcaniclastic sedimentation in lacustrine settings, 1st edn. Blackwell Science, Oxford, pp 83–108

Chen S, Guo ZJ, Pe-Piper G, Zhu BB (2013) Late Paleozoic peperites in West Junggar, China, and how they constrain regional tectonic and palaeoenvironmental setting. Gondwana Res 23:666–681. https://doi.org/10.1016/j.gr.2012.04.012

Conoco C (1987) Geological map of Egypt. Scale 1: 500 000, sheet Cairo

Dadd KA, Van Wagoner NA (2002) Magma composition and viscosity as controls on peperite texture: an example from Passamaquoddy Bay, southeastern Canada. In: Skilling, I.P., White, J.D.L., McPhie, J. (Eds.), Peperite: processes and products of magma-sediment mingling. J Volcanol Geotherm Res 114:63–80. https://doi.org/10.1016/S0377-0273(01)00288-8

De Goër A (2000) Peperites from the Limagne trench (Auvergne, French Massif Central): distinctive facies of phreatomagmatic pyroclastics. History of a semantic drift. In: Leyrit H, Montenat C (eds) Volcaniclastic rocks from magmas to sediments. Gordon and Breach Science Publishers, Amsterdam, pp 91–110

Doyle MG (2000) Clast shape and textural associations in peperite as a guide to hydromagmatic interactions: Upper Permian basaltic and basaltic andesite examples from Kiama, Australia. Aust J Earth Sci 47:167–177. https://doi.org/10.1046/j.1440-0952.2000.00773.x

El-Desoky HM, Khalil AE, Afifl AA (2015) Geochemical and petrological characteristics of the high-Fe basalts from the Northern Eastern Desert, Egypt: abrupt transition from tholeiitic to mildly alkaline flow-derived basalts. Nature & Science 13(6):109–132. https://doi.org/10.7537/marsnsj140816.22

Embabi NS (2018) Climatic conditions: present and past In: Embabi NS, (ed) Landscapes and landforms of Egypt, World geomorphological landscapes. Springer International Publishing AG, pp 25–36. https://doi.org/10.1007/978-3-319-65661-8

Erkül F, Helvacı C, Sözbilir H (2006) Olivine basalt and trachyandesite peperites formed at the subsurface/surface interface of a semi-arid lake: an example from the Early Miocene Bigadiç basin, Western Turkey. J Volcanol Geotherm Res 149(3–4):240–262. https://doi.org/10.1016/j.jvolgeores.2005.07.016

Fedo CM, Nesbitt HW, Young GM (1995) Unraveling the effects of potassium metasomatism in sedimentary rocks and paleosols, with implications for paleoweathering conditions and provenance. Geology 23(10):921–924. https://doi.org/10.1130/0091-7613(1995)023<0921:UTEOPM>2.3.CO;2

Goto Y, McPhie J (1996) A Miocene basanite peperitic dyke at Stanley, northwestern Tasmania, Australia. J Volcanol Geotherm Res 74:111–120. https://doi.org/10.1016/S0377-0273(96)00043-1

Hanson RE, Hargrove US (1999) Processes of magma/wet sediment interaction in a large-scale Jurassic andesitic peperite complex, northern Sierra Nevada. California Bull Volcanol 60:610–626. https://doi.org/10.1007/s004450050255

Hanson RE, Schweickert RA (1982) Chilling and brecciation of a Devonian rhyolite sill intruded into wet sediments, northern Sierra Nevada, California. J Geol 90:717–724. https://doi.org/10.1086/628726

Heikal MTS, Lebda E-MM, Orihashi Y, Habtoor A (2012) Petrogenetic evolution of basaltic lavas from Balhaf–Bir Ali Plio-Quaternary volcanic field, Arabian Sea, Republic of Yemen. Arab J Geosci 7(1):69–86. https://doi.org/10.1007/s12517-012-0726-z

Hunns SR, McPhie J (1999) Pumiceous peperite in a submarine volcanic succession at Mount Chalmers, Queensland, Australia. J Volcanol Geotherm Res 88:239–254. https://doi.org/10.1016/S0377-0273(99)00015-3

Hassaan MM, El-Sheshtawy YA, Hassaan MY, Al-Ashkar A (2004) Basalt: an alternative to shales in cement industry. Applied Mineralogy, Pecchio et al. (eds) ICAM-BR, São Paulo, ISBN 85-98656-01-1

Issawi B, El-Hennawi M, Mazhar A (1999) The Phanerozoic geology of Egypt: a geodynamic approach. Geol Surv Egypt. Special published No. 76, 462p

Jerram D, Stollhofen H (2002) Lava/sediment interaction in desert settings: are all peperite-like textures the result of magma-water interaction? In: Skilling IP, White JDL, McPhie J (eds) Peperite: processes and products of magma- sediment mingling, J Volcanol Geotherm res, vol 114, pp 231–249

Kano K (2002) Middle Miocene volcaniclastic dikes at Kukedo, Shimane Peninsula, SW Japan: fluidization of volcaniclastic beds by emplacement of synvolcanic andesitic dikes. In: Skilling, I.P., White, J.D.L., McPhie, J. (Eds.), Peperite: processes and products of magma-sediment mingling. J Volcanol Geotherm Res 114:81–94

Kano KI (1989) Interaction between andesitic magma and poorly consolidated sediments: examples in the Neogene Shirahama Group, South

Izu, Japan. J Volcanol Geotherm Res 37:59–75. https://doi.org/10.1016/0377-0273(89)90113-3

Kokelaar BP (1982) Fluidization of wet sediments during the emplacement and cooling of various igneous bodies. J Geol Soc Lond 139: 21–33 https://doi.org/10.1144/gsjgs.139.1.0021

Kokelaar BP (1986) Magma water interactions in subaqueous and emergent basaltic volcanism. Bull Volcanol 48:275–289. https://doi.org/10.1007/BF01081756

Leat PT (1985) Interaction of a rheomorphic peralkaline ash-flow tuff and underlying deposits, Menengai Volcano, Kenya. J Volcanol Geotherm Res 26:131–145. https://doi.org/10.1016/0377-0273(85)90049-6

Martin U, Németh K (2007) Blocky versus fluidal peperite textures developed in volcanic conduits, vents and crater lakes of phreatomagmatic volcanoes in Mio/Pliocene volcanic fields of Western Hungary. J Volcanol Geotherm Res 159(1–3):164–178. https://doi.org/10.1016/j.jvolgeores.2006.06.010

McLean CE, Brown DJ, Rawcliffe HJ (2016) Extensive soft-sediment deformation and peperite formation at the base of a rhyolite lava: Owyhee Mountains, SW Idaho, USA. Bull Volcanol 78(6):1–17. https://doi.org/10.1007/s00445-016-1035-2

McPhie J (1993) The Tennant Creek porphyry revisited: a synsedimentary sill with peperite margins, early Proterozoic, Northern Territory. Aust J Earth Sci 40:545–558. https://doi.org/10.1080/08120099308728103

Meneisy MY, Abdel Aal AY (1983) Geochronology of Phanerozoic volcanic activity in Egypt. Ain Shams Science Bull 25(24):163–175

Moustafa AR, Abd-Allah AMA (1991) Structural setting of the central part of the Cairo- Suez district-Mid East Res. Cent., Ain Shams Univ. Sc Res Ser 5 :133–145

Németh K, Martin U (1999) Large hydrovolcanic field in the Pannonian Basin: general characteristics of the Bakony-Balaton Highland Volcanic Field, Hungary. Acta Vulcanol 11(2):271–282

Németh K, White CM (2009) Intra-vent peperites related to the phreatomagmatic 71 Gulch Volcano, western Snake River Plain volcanic field, Idaho (USA). J Volcanol Geotherm Res 183(1–2):30–41. https://doi.org/10.1016/j.jvolgeores.2009.02.020

Pearce JA (1983) Role of sub-continental lithosphere in magma genesis at active continental margins. In: Norry MJ (ed) Hawkes worth CJ. Continental basalts and mantle xenoliths. Shiva, Cheshire, pp 230–249

Rawlings DJ, Watkeys MK, Sweeney RJ (1999) Peperitic upper margin of an invasive £ow, Karoo flood basalt province, northern Lebombo. S Afr J Geol 102:377–383 https://hdl.handle.net/10520/EJC-942c9cf52

Said R (1990) Cenozoic. In: Said R (ed) The geology of Egypt. Balkema, Rotterdam, pp 451–486

Schmincke HU (1967) Fused tuffs and peperites in south-central Washington. Geol Soc Am Bull 78:319–330

Schipper CI, White JDL, Zimanowski B, Büttner R, Sonder I, Schmid A (2011) Experimental interaction of magma and “dirty” coolants. Earth planet. Sci. Lett. 303:232–336. https://doi.org/10.1016/j.epsl.2011.01.010

Skilling IP, White JDL, McPhie J (2002) Peperite: a review of magma–sediment mingling. J Volcanol Geotherm Res 114:1–17. https://doi.org/10.1016/S0377-0273(01)00278-5

White JDL, McPhie J, Skilling I. P (2000) Peperite: a useful genetic term. Bull Volcanol 62:65–66. https://doi.org/10.1007/s0044500502

Wohletz K (2002) Water/magma interaction: some theory and experiments on peperite formation. J Volcanol Geotherm Res 114(1–2): 19–35. https://doi.org/10.1016/S0377-0273(01)00280-3

Zimanowski B, Buttner R (2002) Dynamic mingling of magma and liquefied sediments. J Volcanol Geotherm Res 114(1–2):37–44. https://doi.org/10.1016/S0377-0273(01)00281-5